ICANS-XI International Collaboration on Advanced Neutron Sources
KEK, Tsukuba, October 22-26, 1990

IMPROVING THE RESOLUTION OF CHOPPER SPECTROMETERS AT PULSED NEUTRON SOURCES

J. M. Carpenter
Intense Pulsed Neutron Source, Argonne National Laboratory,
9700 South Cass Avenue, Argonne IL 60439
and
D. F. R. Mildner
Center for Analytical Chemistry
National Institute of Standards and Technology,
Gaithersburg MD 20899

ABSTRACT

We examine the relationships between intensity and resolution in pulsed-source chopper spectrometers, including the effects of Soller collimation, narrower rotor slits and higher rotor speeds. The basis is a simplified description of a spectrometer, approximately optimizing the rotor pulse and lighthouse effects. The analysis includes a new treatment of the angular distribution transmitted through a system consisting of a coarse collimator and a Soller collimator. The results encourage the prospect for a reasonably easily accomplished, higher resolution, optional configuration of the pulsed source chopper spectrometers at IPNS.

I. INTRODUCTION

All three chopper spectrometers[1] at IPNS[2] include Soller collimation between the incident beam monitor detector, which is immediately downstream from the chopper, and the sample. This is primarily a shielding device which has little impact on the resolution or intensity of the instrument.

Here we consider the Soller collimator as a device to narrow the angular distribution of the beam striking the sample, and thus to reduce that contribution (sometimes called the "lighthouse" or the "sweep time" effect) to the chopped-beam pulse width and to the resolution of the instrument. A similar effect can be obtained by narrowing the width of the slits in the chopper, though in this case the limit of what can be done approaches the pulse width due to the lighthouse effect. This can also be accomplished by increasing the rotor angular speed as has been done at the HET and MARI spectrometers[3] at ISIS, but this would require major modifications to the rotor systems of the IPNS instruments. The object of this work is to examine the effects on the intensity and the resolution caused by adjusting the Soller collimation and the chopper slit width,

optimizing the combined effects under the constraints of fixed rotor speed, rotor aperture, and moderator size.

In the process we find it necessary to calculate the angular distribution of neutrons transmitted by two overlaid collimating systems, one coarse (defined by the widths and separation of the moderator, the rotor aperture and the sample) and one fine (defined by the Soller collimator). The present work complements that of Loong, Ikeda and Carpenter[4] in this respect.

II. Intensity and Resolution

Figure 1 schematically represents the components of the spectrometer. Throughout, it is assumed that the collimator is wider than the penumbra of the beam formed by the source and the chopper. The time-averaged number of neutrons passing through the system per unit time is

$$I(E) = (2E_1/t_1)\, i(E)\, C\Delta\Omega f_R f_C \Delta t_R$$

$$= 2 i_{epi} C\Delta\Omega f_R f_C v_1 \Delta t_R / L_1, \qquad (1)$$

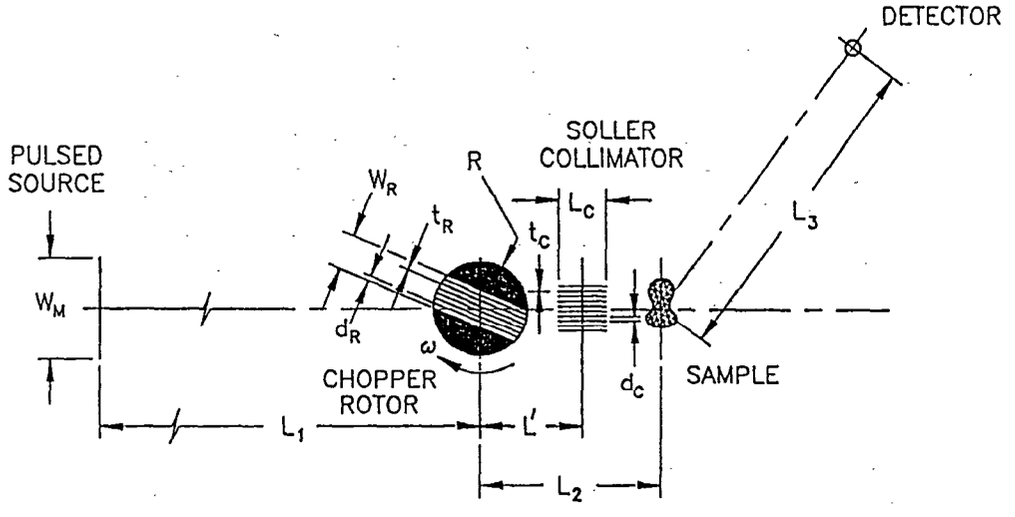

Figure 1: A schematic diagram of the time-of-flight chopper spectrometer on a pulsed neutron source. The pulsed source is the moderator of width W_M. The chopper of radius R is located a distance L_1 downstream and is rotating at an angular speed ω; it has an aperture of width W_R which includes numerous neutron-opaque slats of width t_R, spaced d_R apart. Located a further distance L' downstream is a Soller collimator of length L_C with numerous neutron-opaque slats of width t_C, spaced d_C apart. The sample is located a distance L_2 from the rotor, and the detector is a distance L_3 from the sample.

where i(E) is the time-averaged beam current per unit energy, that is, the number of neutrons per unit time, per unit energy, per unit solid angle, emitted from the entire moderator surface. $2E_1/t_1$ is the Jacobian $|dE/dt|$. $i_{epi} = Ei(E)$ is approximately constant with respect to E in the epithermal region. $C\Delta\Omega$ is the solid angle accepted from an average point on the moderator surface, C is a factor which represents the fraction of the source area viewed, f_R and f_C are the fractions of the areas of the rotor aperture and the collimator that are open,

and Δt_R is the rotor pulse width for a perfectly collimated beam. The subscript 1 refers to the beam from the moderator incident on the chopper rotor.

If there is no Soller collimator, the accepted solid angle is given by

$$C\Delta\Omega = H_R W_R / L_1^2, \tag{2}$$

where H_R and W_R are the height and width of the chopper aperture, and L_1 is the distance between the source and the chopper centerline. The more general situation represented by Figure 1 is rather complicated. The main burden of this work is to analyze this case.

Consider a Soller collimator whose angular divergence α_C is given by

$$\alpha_C = d_C / L_C, \tag{3}$$

where d_C is the width of the collimator slits of length L_C. Let the collimator divergence be very small, viz., $\alpha_C << W_M/L_1$ and $\alpha_C << W_R/L_1$, where W_M is the width of the source (moderator). The accepted solid angle is now

$$\Delta\Omega = H_R \alpha_C / L_1, \tag{4}$$

and the viewing factor is

$$C = \begin{cases} W_R/W_M & \text{if } W_R \le W_M \\ 1 & \text{if } W_R \ge W_M. \end{cases} \tag{5}$$

(See equation (A17) in the Appendix.)

The duration of the rotor pulse (the full width at half-maximum in a perfectly collimated beam) for neutrons of optimum speed is

$$\Delta t_R = d_R / (2R\omega), \tag{6}$$

where d_R is the rotor slit width, R is the radius of the slit package, and ω is the rotor angular speed. The fractions are

$$f_R = d_R/(d_R + t_R), \quad f_C = d_C/(d_C + t_C) \tag{7), (8}$$

where t_R and t_C are the thicknesses of the slats.

The energy transfer resolution (neglecting the effects of sample size, detector thickness, and time channel width) is[4]

$$\sigma_e^2 = (m^2/L_1^2)\{[v_1^3 + (L_2/L_3)v_2^3]^2\sigma_t^2 + [v_1^3 + ((L_1 + L_2)/L_3)v_2^3]^2\sigma_C^2\}, \tag{9}$$

where m is the neutron mass, v_1 and v_2 are the incident and scattered neutron speeds, and σ_e^2, σ_t^2, and σ_C^2 are respectively the variances of the energy transfer, moderator emission time and chopper pulse time distributions. L_2 and L_3 are the distances from the chopper to the sample, and from the sample to the detector, respectively.

In the epithermal regime, the standard deviation of the moderator emission time t is given by

$$\sigma_t = \sqrt{3}/(av_1), \tag{10}$$

where a is the constant in the moderator emission time distribution[3],

$$\phi(v,t) \propto t^2 e^{-avt}. \tag{11}$$

The chopper pulse variance is

$$\sigma_C^2 = \sigma_R^2 + \sigma_L^2, \tag{12}$$

where σ_R is the standard deviation of the (triangular) rotor pulse for neutrons of optimum speed in a perfectly collimated beam,

$$\sigma_R^2 = (\Delta t_R)^2/6. \tag{13}$$

σ_L is the contribution to the chopper pulse width due to the lighthouse effect,

$$\sigma_L = \sigma_\alpha/\omega, \tag{14}$$

where σ_α is the standard deviation of the angular distribution of the neutrons transmitted through the system.

It is shown in the Appendix that if there is no Soller collimator, the angular acceptance is

$$\Delta\alpha = \psi_0 + \psi_1 \tag{15}$$

and the variance of the distribution is

$$\sigma_\alpha^2 = (\psi_0^2 + \psi_1^2)/6, \tag{16}$$

where

$$\psi_0 = (W_M + W_R)/(2L_1) \tag{17}$$

and

$$\psi_1 = |W_M - W_R|/(2L_1). \tag{18}$$

On the other hand, if the Soller collimator completely determines the angular distribution, then

$$\Delta\alpha = \alpha_C = d_C/L_C \tag{19}$$

and

$$\sigma_\alpha^2 = (\Delta\alpha)^2/6 = \alpha_C^2/6, \tag{20}$$

where d_C and L_C are the width and length of the collimator slits.

The expressions for $\Delta\alpha$ and σ_α for a partially illuminated collimator are more complicated, and are set out below and in the Appendix. The full width at

half maximum (FWHM) is used as the estimate of resolution. The relationship between the FWHM and the standard deviation of the distribution of any quantity q is given by $\Delta q = \sqrt{(8\ln 2)}\sigma_q = 2.35\sigma_q$ applies if q has a Gaussian distribution; we use this relationship even though it is only approximately true.

III. APPROXIMATE OPTIMIZATION

The transmitted intensity is proportional to the product of the angular acceptance and the rotor pulse width,

$$I \propto \Delta\alpha\Delta t_R, \tag{21}$$

and the energy transfer resolution depends on the time and angular variances (see equations (9), (12) and (14))

$$\sigma_\epsilon^2 = A + B(\sigma_R^2 + \sigma_\alpha^2/\omega^2). \tag{22}$$

(We need not be explicit about the factors A and B here.) An approximate optimization results if we assume that the variances are related in identical proportion to the the full widths at half maximum, for example, as they are for triangular distributions (see equations (13) and (20), though neither of these is generally true). Then the greatest intensity for some given energy transfer resolution is attained when $\Delta t_R = \Delta\alpha/\omega$, or

$$\sigma_R = \sigma_\alpha/\omega. \tag{23}$$

The calculations performed as an initial approximation and for survey purposes assume this relationship. To the extent that it is incorrect, the calculated intensity is smaller than could actually be obtained for the same resolution, therefore a second pass optimization has to be performed, using the more accurate relationships. If the Soller collimation completely determines the angular distribution, and the neutrons are of optimum speed for the rotor, the expressions (13) and (20) are exact, and the optimization equation (23) is also exact.

IV. THE ANGULAR DISTRIBUTION OF ACCEPTED NEUTRONS

The angular distribution of neutrons transmitted through a partially illuminated Soller collimator depends in a complicated way upon the parameters of the system. However, ignoring the fine structure of the spatial and angular distribution, the angular distribution $P(\psi)$ can be expressed as

$$P(\psi) = F_R(\psi)F_C(\psi), \tag{27}$$

where $F_R(\psi)$ describes the angular distribution that would be transmitted through the rotor aperture from the moderator surface, and $F_C(\psi)$ describes the angular distribution that would be transmitted through a fully illuminated collimator slit which is assumed to be much smaller than the rotor aperture. Figure 2 illustrates the distributions $P(\psi)$, $F_R(\psi)$, and $F_C(\psi)$; these may be deduced from Figure A3 in the Appendix which shows the phase space diagram at the collimator center.

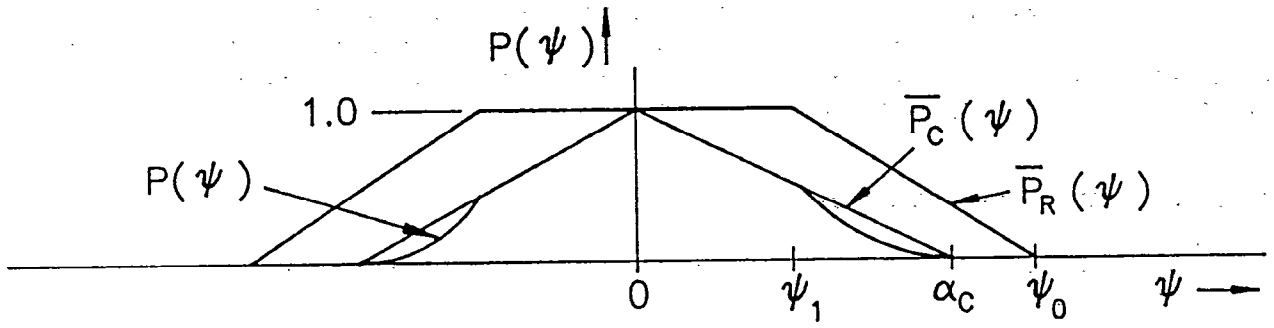

Figure 2: *The angular distribution $F_R(\psi)$ of neutrons transmitted through the rotor aperture from the moderator surface, and the angular distribution $F_C(\psi)$ of neutrons that would be transmitted through a fully illuminated collimator slit. Their product $P(\psi)$ gives the angular distribution of neutrons transmitted through a partially illuminated collimator. The results shown are for the case $\psi_1 < \alpha_C < \psi_0$, and may be deduced from Figure A3 in the Appendix.*

In the Appendix we develop an expression for the number of neutrons passing through the system per unit time (equation (1)) in terms of the distributions given by the approximation (27), and introduce the viewing factor C (equations (5) and (A17)). The results give

$$F_R(\psi) = \begin{cases} 1, & 0 < |\psi| < \psi_1 \\ (\psi_0 - |\psi|)/(\psi_0 - \psi_1), & \psi_1 < |\psi| < \psi_0 \\ 0, & |\psi| > \psi_0, \end{cases} \tag{28}$$

and

$$F_C(\psi) = \begin{cases} 1 - |\psi|/\alpha_C, & 0 < |\psi| < \alpha_C \\ 0, & |\psi| > \alpha_C. \end{cases} \tag{29}$$

There are several cases for $P(\psi)$, depending upon the relative values of α_C, ψ_0, and ψ_1. Figure 2 is for the case $\psi_1 < \alpha_C < \psi_0$. The angular acceptance and the variance of the distribution are given by

$$\Delta\alpha = \int_{-\infty}^{\infty} P(\psi)\,d\psi \tag{30}$$

and

$$\sigma_\alpha^2 = (1/\Delta\alpha)\int_{-\infty}^{\infty} \psi^2 P(\psi)\,d\psi. \tag{31}$$

For $\alpha_C < \psi_1$, we have

$$\Delta\alpha = \alpha_C \tag{32}$$

and

$$\sigma_\alpha^2 = \alpha_C^2/6. \tag{33}$$

For this condition, the expression (20) is exact, and the optimization equation (23) is also exact for neutrons of optimum speed for the rotor.

For $\psi_1 < \alpha_C < \psi_0$,

$$\Delta\alpha = 2\{\psi_1(1 - \psi_1/(2\alpha_C)) + (1/(\psi_0 - \psi_1))[(\alpha_C - \psi_1)\psi_0 - (\alpha_C^2 - \psi_1^2)(1 + \psi_0/\alpha_C)/2 + (\alpha_C^3 - \psi_1^3)/(3\alpha_C)]\}, \quad (34)$$

and

$$\sigma_\alpha^2 = (2/\Delta\alpha)\{\psi_1^3(1/3 - \psi_1/(4\alpha_C)) + (1/(\psi_0 - \psi_1))[(\alpha_C^3 - \psi_1^3)\psi_0/3 - (\alpha_C^4 - \psi_1^4)(1 + \psi_0/\alpha_C)/4 + (\alpha_C^5 - \psi_1^5)/(5\alpha_C)]\}. \quad (35)$$

For $\alpha_C > \psi_0$,

$$\Delta\alpha = 2\{\psi_1(1 - \psi_1/(2\alpha_C) + (1/(\psi_0 - \psi_1))[(\psi_0 - \psi_1)\psi_0 - (\psi_0^2 - \psi_1^2)(1 + \psi_0/\alpha_C)/2 + (\psi_0^3 - \psi_1^3)/(3\alpha_C)]\}, \quad (36)$$

and

$$\sigma_\alpha^2 = (2/\Delta\alpha)\{\psi_1^3(1/3 - \psi_1/(4\alpha_C)) + (1/(\psi_0 - \psi_1))[(\psi_0^3 - \psi_1^3)\psi_0/3 - (\psi_0^4 - \psi_1^4)(1 + \psi_0/\alpha_C)/4 + (\psi_0^5 - \psi_1^5)/(5\alpha_C)]\}. \quad (37)$$

No simple analytic expressions relating the angular acceptance $\Delta\alpha$ and the variance σ_α^2 of the angular distribution can be obtained for these last two conditions.

In the limit of very large α_C, equations (36) and (37) become the simple results already known for the case with no Soller collimator,

$$\Delta\alpha = \psi_0 + \psi_1 \quad (15)$$

and

$$\sigma_\alpha^2 = (\psi_0^2 + \psi_1^2)/6. \quad (16)$$

V. Calculations

We have performed several calculations all of which correspond to the flight path lengths of the HRMECS instrument[1] at IPNS. The thickness of the collimator blades is neglected so that $f_C = 1$. Table I shows the cases calculated.

Cases 1 and 2 correspond to current IPNS rotor technology[1]; case 3 represents HRMECS with a chopper similar to that[5] currently proposed for the Los Alamos Neutron Scattering Center (LANSCE) chopper spectrometer; case 4 is for HRMECS with a chopper similar to that of the HET spectrometer at ISIS. All cases were computed with the approximate optimization condition (23) for small rotor slit spacings, for which a Soller collimator is appropriate for optimum

intensity. For larger rotor slit spacings, highest intensity demands no Soller collimator, and the calculations do not include the effect of Soller collimation.

Figure 3 illustrates the results of these calculations for case 1, that of the HRMECS instrument with a standard 3" x 4" rotor of radius 77 mm at a frequency of 270 Hz and an incident energy E_1 of 500 meV. Shown in this Figure are the time-averaged neutron intensity $I(E_1)$ transmitted per unit time, the optimized collimation α_C, the chopper pulse FWHM Δt_C (including the lighthouse effect, and given by equation (12)), the FWHM energy transfer resolution for elastic scattering Δe_{el}, and the FWHM

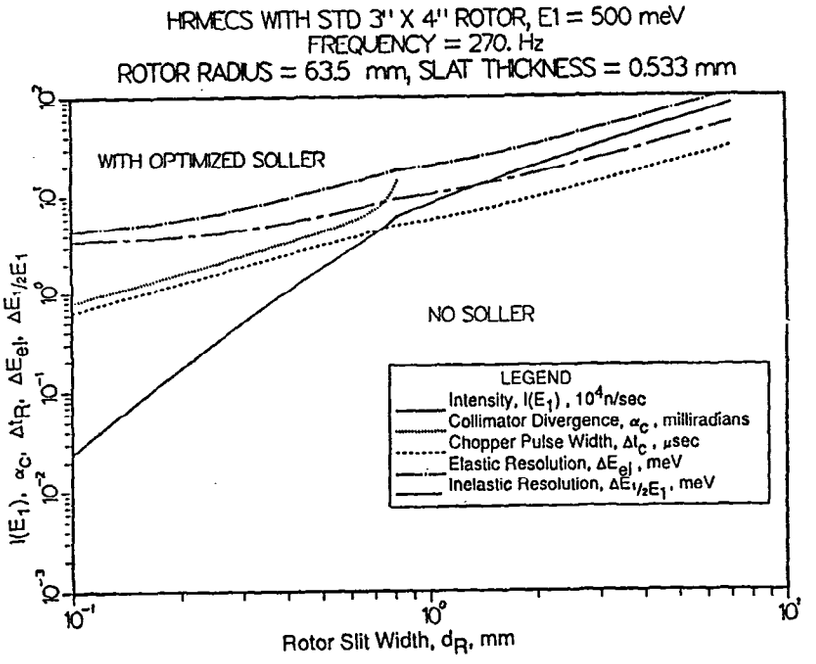

Figure 3: The results of the optimized intensity calculations as a function of rotor slit width d_R for the HRMECS instrument with a 3" x 4" rotor of radius 77 mm at a frequency of 270 Hz and an incident energy E_1 of 500 meV. Plotted are the time-averaged neutron intensity $I(E_1)$ transmitted per unit time, the collimation α_C the chopper pulse FWHM Δt_C, the FWHM energy transfer resolution for elastic scattering Δe_{el}, and the FWHM energy transfer resolution for loss of one-half the incident energy $\Delta e_{(1/2E1)}$.

energy transfer resolution for loss of one-half the incident energy $\Delta e_{(1/2E1)}$, all plotted as functions of the rotor slit width d_R. Also shown on Figure 3 are plotted points which correspond to calculations for the currently-used Soller collimator of HRMECS, namely α_C = 11.6 mrad, and for the rotor slit widths of the normal and high-resolution rotors without the optimization condition. As the rotor slit width approaches zero, the chopper pulse width approaches its limit Δt_L defined by the lighthouse effect, the energy transfer resolutions approach their minimum values, but also the transmitted intensity approaches zero. For larger slit widths, all these values increase.

TABLE I

The specifications for different rotor types used in the calculations. W_M is the moderator width, E_I the incident energy, ν the rotor frequency, R the rotor radius, W_R and H_R the width and height of the chopper aperture, d_R the rotor slit width, and t_R the rotor slat thickness.

Case	Rotor Type	W_M, mm	E_I, meV	ν, Hz	R, mm	W_R, mm	H_R, mm	d_R, mm	t_R, mm
1	IPNS	100.	500.	270.	63.5	76.2	101.6	1.02	0.533
2	IPNS	100.	500.	270.	77.0	50.8	101.6	1.57	0.533
3	LANSCE	100.	500.	600.	50.0	43.2	66.0	0.80	0.660
4	ISIS	100.	500.	600.	50.0	47.0	47.0	0.76	0.380

The other three cases of Table I give results which are similar in form to those shown in Figure 3, though the range over which the Soller collimation is required for the other cases depends on the rotor slit width d_R. The relative intensities for each case should be compared at fixed resolution. Figure 4 represents the same data for case 1 as a function of the elastic energy transfer resolution to facilitate such a comparison. This is possible because the resolution and the rotor slit width are related monotonically. From such figures for each case we have generated Table II which shows the relative intensities at different energy transfer resolutions.

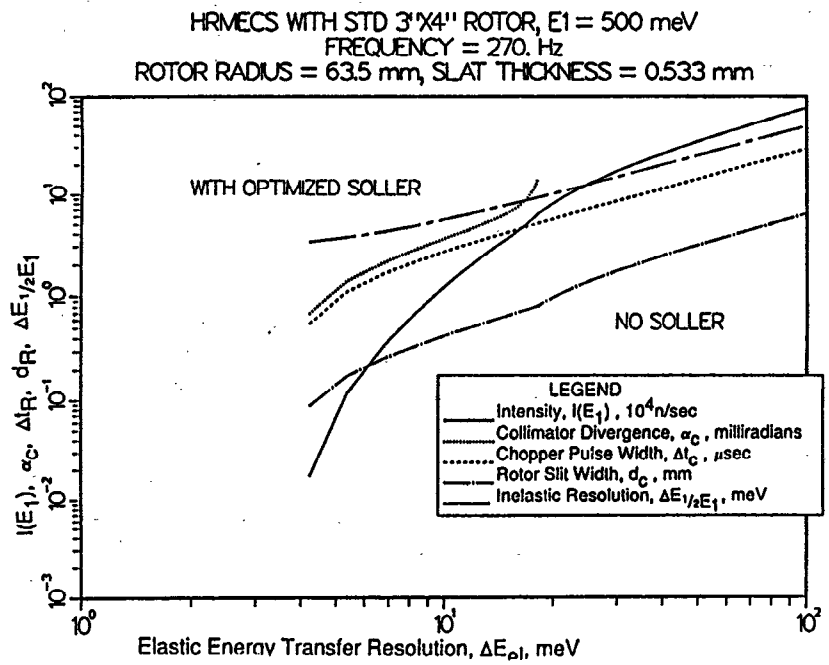

Figure 4: The results of the optimized intensity calculations as a function of the elastic energy transfer resolution $\Delta\epsilon_{el}$ for the HRMECS instrument with a 3" x 4" rotor of radius 77 mm at a frequency of 270 Hz and an incident energy of 500 meV (similar to Figure 3).

TABLE II

The relative intensities at 500 meV (in units of 10^4 cm^{-2} sec^{-1}) for the four different rotor types given in Table I for elastic energy transfer resolutions of 10, 12.5, 15 and 20 meV.

Case	Rotor Type	$\Delta\epsilon_{el}$ = 10 meV	$\Delta\epsilon_{el}$ = 12.5 meV	$\Delta\epsilon_{el}$ = 15 meV	$\Delta\epsilon_{el}$ = 20meV
1	IPNS	1.25	2.1	3.4	8.3
2	IPNS	0.84	1.7	2.7	6.0
3	LANSCE	1.3	2.0	2.8	4.2
4	ISIS	1.3	1.8	2.2	3.4

Recognizing that the condition (23) is only approximate, we have searched for higher intensity conditions with fixed resolution. For example, Figure 5 shows the results for the 270 Hz rotor with a 3"x 4" aperture (case 1) for elastic resolution of 10. meV (2 % of the incident energy for 500. meV incident energy), which is comparable to HET. The approximate optimization gives about the same intensity as the refined optimization, since the intensity varies rather slowly around the optimum. Various choices of α_C and d_R that give the same resolution also give almost the same intensity. The intensity and the approximately optimized and refined parameters for this energy transfer resolution are given in Table III. The results for energy transfer resolutions of 12.5 and 15. meV for elastic scattering for the same rotor are given in Table III. The Figures from which these results are derived are similar in shape as those shown in Figure 5. For comparison, Table III also gives the intensity and the parameters for the present HRMECS arrangement, for which the elastic resolution is calculated to be about 20. meV. (The calculated results for the present arrangement are close to observed values.) The Table also gives parameters for HRMECS with a 600 Hz rotor similar to that for the ISIS HET spectrometer, and with no Soller collimator. All these results include the effect of the partial open area of rotor slit package, $f_R = d_R/(d_R + t_R)$.

The intensity loss for 12.5 meV resolution compared to present rotor design is only about a factor of 3.5, which is now nearly compensated by the increased intensity available from the IPNS booster target[6]. The parameters appear to be feasible. The reason that the intensity loss is not greater is that the source pulse width, the rotor, and lighthouse contributions to the resolution are not perfectly optimized in the present HRMECS. The resolution improvement accomplishable by the present method is relatively easy compared to the alternative of replacing existing choppers with magnetic-bearing choppers. It requires only a new rotor and slit package of the same type now in use, and a new Soller collimator. The new arrangement could easily be introduced as an option among other instrument configurations.

Comparing the results of Figure 4 (for HRMECS with a standard, 270 Hz rotor and optimized Soller collimator) with those for HRMECS with an ISIS-style, 600 Hz rotor, we see that for the same resolution, the standard rotor provides the same or <u>better</u> intensity for given resolution. This is because the aperture of the standard rotor is larger than that of the ISIS rotor. This conclusion must be

TABLE III

The calculated transmitted intensity $I(E_1)$ at an incident energy E_1 of 500 meV and the rotor and collimator parameters (chopper pulse width Δt_C, rotor pulse width Δt_R, rotor slit width d_R and Soller collimation α_C) for both the approximately optimized and the refined cases for the HRMECS rotor design (270 Hz), optimized for different energy transfer resolutions $\Delta\epsilon_{el}$ and $\Delta\epsilon_{1/2El}$ with the HRMECS flight path arrangement. Also shown are the present arrangement for HRMECS, and that for the 600 Hz HET rotor with the HRMECS spectrometer design.

	$\Delta\epsilon_{el}$ meV	$\Delta\epsilon_{1/2El}$ meV	$I(E_1)$ n/sec	Δt_C μsec	Δt_R μsec	d_R mm	α_C mrad
Approx. opt.(1)	10.0	5.63	1.24	2.70	1.99	0.428	3.63
Refined opt.(1)	10.0	5.63	1.29	2.70	2.19	0.473	3.15
Approx. opt.	12.5	6.76	2.31	3.47	2.56	0.551	4.93
Refined opt.	12.5	6.76	2.38	3.47	2.82	0.606	4.25
Approx. opt.	15.0	7.92	3.70	4.23	3.12	0.671	6.57
Refined opt.	15.0	7.92	3.80	4.23	3.44	0.740	5.45
HERMECS #	20.1	10.4	8.22	5.76	4.73	1.02	11.6
With HET chopper*,	9.3	5.34	1.27	2.49	2.02	0.760	----

(1) corresponding to Figure 5
\# present arrangement
* with no Soller collimator

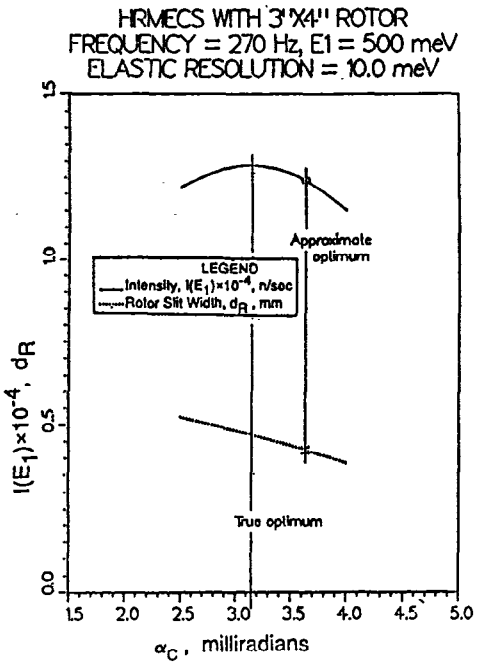

Figure 5: ***The results of the more refined optimization for an elastic energy transfer resolution*** $\Delta\epsilon_{el}$ ***of 10.0 meV for the HRMECS 3" x 4" rotor of radius 77 mm at a frequency of 270 Hz with an incident energy*** E_1 ***of 500 meV (similar to Figure 3), showing the intensity*** $I(E_1)$ ***transmitted and the rotor slit width*** d_R ***as a function of the collimation*** α_C.

tempered, however, by the realization that sample size contributions to the resolution are not accounted for in these comparisons; these are smaller in the case of the ISIS rotor, but can be focussed out for special conditions.

Finally, we repeat that all calculations assume that the collimator open fraction $f_C = 1$, that is, we have ignored the thickness of the collimator blades (thus we have avoided being specific about the length of the collimator and the width of the slits). In practice, we caution that this factor must be included in final design calculations; it can readily be introduced at the stage represented by Figure 5, as a factor on the intensity given there.

VII. Conclusions

We have further developed the relationships between the resolution and intensity for time-of-flight chopper spectrometers, including the effect of Soller collimation. The angular distribution is determined coarsely by the size of the moderator and the rotor aperture, together with the distance separating them, and is resolved finely by the Soller collimation. The placing of additional collimation between the chopper and the sample reduces the angular distribution of the beam striking the sample, and hence reduces the lighthouse contribution to the instrumental resolution. We have considered the effects of adjusting this collimation and the chopper slit width, assuming a fixed rotor speed, rotor aperture and moderator size, and have optimized the rotor pulse and the lighthouse effect for the best intensity. The transmitted intensity is

proportional to the product of the angular acceptance and the rotor pulse width. The energy transfer resolution depends on the root of the sums of squares of the rotor pulse width and the lighthouse effect (the angular acceptance of the system divided by the rotor angular speed). The greatest intensity for some given energy transfer resolution occurs when these two quantities are equal.

We have derived new expressions for the angular distribution of a beam formed by a coarse collimator system overlaid by a fine Soller collimator, assuming that the collimator slit width is much less than the widths of the moderator and the rotor aperture. Slightly different expressions are obtained depending on the relative sizes of the moderator and the rotor aperture. This distinction determines whether the collimator lies in the umbra of the beam (the source is fully observable through the rotor aperture), or whether the center of the beam in penumbra (the source is partially obscured by the rotor aperture). We have considered the optimized conditions for no collimation present, for Soller collimation placed between the rotor and the sample, and when the collimation is only partially illuminated. We show that small rotor slit spacings require appropriate Soller collimation for optimum intensity, whereas for large rotor slit spacings the highest intensity requires no Soller collimation.

VIII. APPENDIX

The angular and spatial distribution of neutrons transmitted through a collimating system in two dimensions can be usefully described in terms of diagrams in the phase space consisting of the positions and directions of trajectories at their crossing of a reference screen, which will be placed at the collimator center. Figure A1 illustrates the definitions of relevant quantities. A neutron which leaves from the point (z',ψ') in the source phase space, at a position z' in the source plane and in direction ψ' relative to the reference axis, crosses a reference screen at a distance L along and normal to the reference axis of the beam at a point (z,ψ) in its phase space given by

$$z = z' + L\psi'$$

$$\psi = \psi' \qquad \text{(A1)}$$

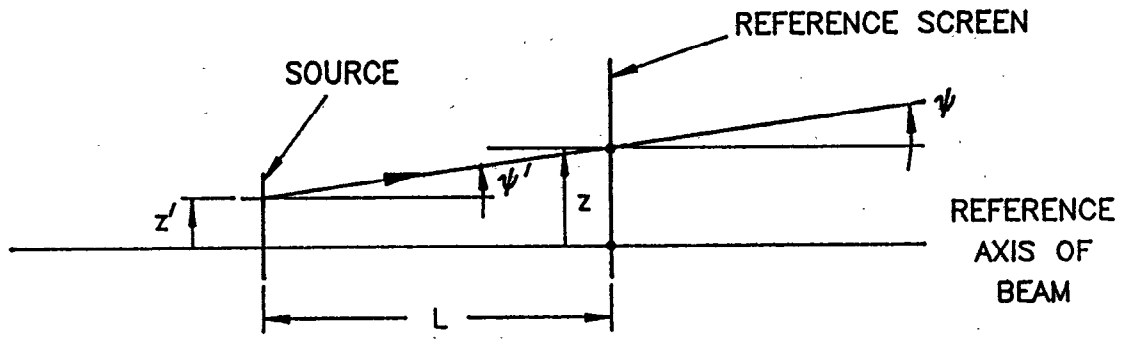

Figure A1: *A neutron leaves the source from a point (z',ψ') in the source phase space, where z' is the distance from the reference axis of the beam, and ψ' is the direction relative to that axis. The neutron traces a path which crosses a*

reference screen placed a distance L along and normal to the reference axis at a point (z,ψ) in the reference plane phase space, such that $z = z' + L\psi'$ and $\psi = \psi'$.

In the case under consideration, we need to describe the combined effect of a finite, isotropic source (the moderator), a finite aperture (the chopper), and a Soller collimator. Figure A2 shows the horizontal plane of the geometry of the collimation system considered in this paper. The reference screen is taken as the collimator centerline, and Figure A3 shows the corresponding phase space acceptance diagram. Everything is represented and calculated in the sense of small angle approximations, and for the purpose of this Appendix in two dimensions.

The areas inside the parallelograms are regions of the phase space that are illuminated by the source and accepted through the system. The large shaded parallelogram where $P_R(z,\psi) = 1$ represents the region illuminated by the finite source that is accepted through the rotor aperture, and the small parallelograms where $P_C(z,\psi) = 1$ represent the region that is accepted through the Soller collimator. Altogether, the region illuminated and accepted by the system depicted in Figure A2 is the region common to both the large and the small parallelograms.

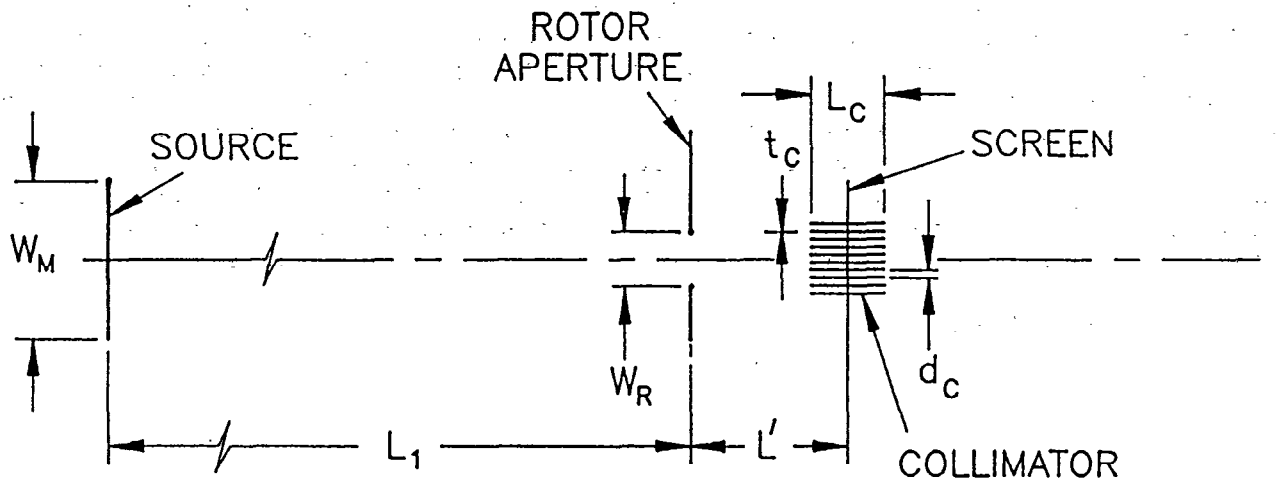

Figure A2: A schematic diagram of the horizontal plane of the geometry of the collimation system. The moderator has a width W_M. The chopper has an aperture width W_R and its centerline is located L_1 downstream. The Soller collimator of length L_C has slits of width d_C and slats of width t_C, and its centerline is located a further distance L' beyond the chopper. The reference screen for Figure A3 is taken as the collimator centerline.

The lines $z = (L_1 + L')\psi \pm W_M/2$ represent the boundaries of the region in phase space illuminated by the moderator. The lines $z = L'\psi \pm W_R/2$ represent the boundaries of the region transmitted by the rotor aperture. These lines cross at $\pm W_R/2 = L_1\psi \pm W_M/2$. That is,

$$\psi_0 = \pm (W_M + W_R)/(2L_1) \qquad (17)$$

and

$$\psi_1 = \pm \left| W_M - W_R \right| / (2L_1) . \tag{18}$$

The lines $z = \pm L_C\psi/2 \pm d_C/2 + n(d_C + t_C)$ represent the boundaries of the region in phase space transmitted by the n^{th} collimator slit. For each collimator slit, these lines cross at $\psi = 0$ and at $\psi = \pm \alpha_C = \pm d_C/L_C$ (equation (3)). An integration over z for the regions depicted in Figure A3 will give the distributions $\bar{P}_R(\psi)$, $\bar{P}_C(\psi)$ and $P(\psi)$ defined by equations (27).

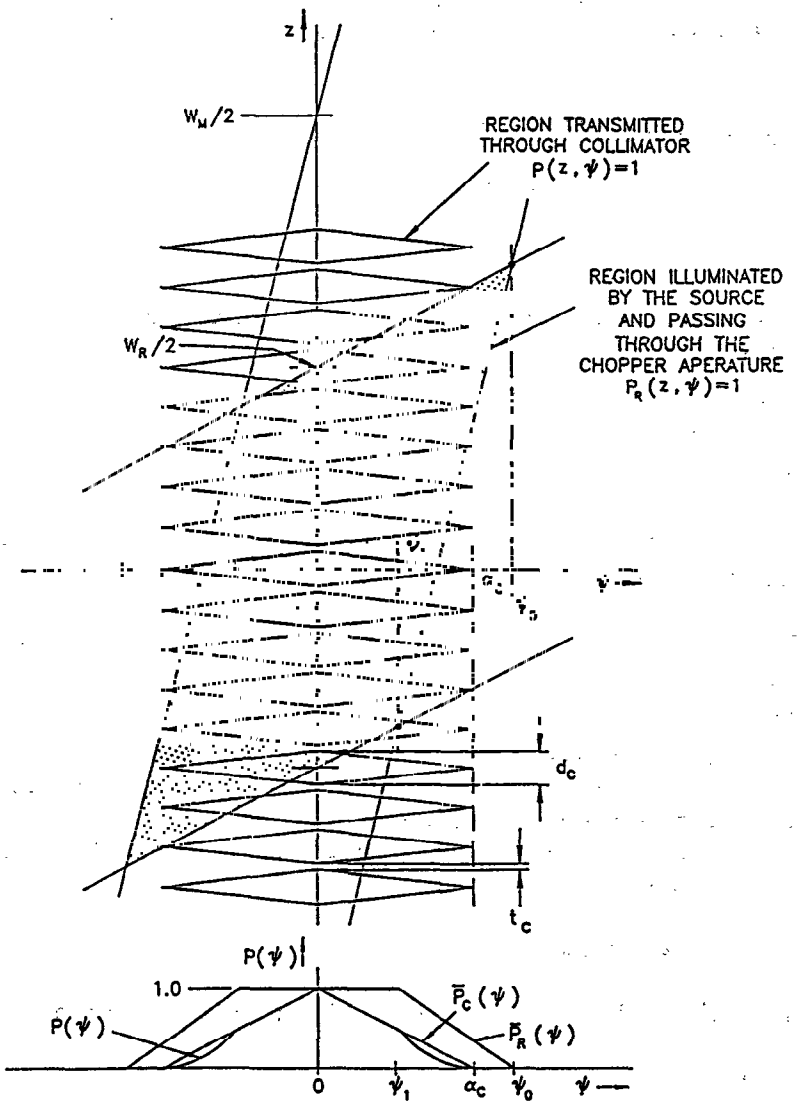

Figure A3: *The phase space acceptance diagram at the collimator centerline for the geometry depicted in Figure A2. The large shaded parallelogram where $P_R(z,\psi) = 1$ represents the region illuminated by the moderator of width W_M, and transmitted by the rotor aperture of width W_R placed at a distance L_1 downstream from the moderator and a distance L′ before the collimator. The small parallelograms where $P_C(z,\psi) = 1$ represent the regions transmitted through each collimator slit of width d_C and length L_C. Those regions common to both correspond to rays transmitted through the system.*

If the angular current density on the source plane is $\phi_s(z',\psi')$, then the number of neutrons passing through the system per unit time is

$$I = \int \phi_s(z',\psi')\ P_R(z,\psi)\ P_C(z,\psi)\ \delta(z - z' - (L_1 + L')\psi)\ \delta(\psi - \psi') \\ dzd\psi dz'd\psi', \tag{A2}$$

where the delta functions represent the transformation (equation (A1) from the phase space at the source to that at the reference screen. Performing the integrals gives

$$I = \int \phi_s(z - (L_1 + L')\psi,\psi)\ P_R(z,\psi)\ P_C(z,\psi)\ dzd\psi. \tag{A3}$$

Assuming that the source angular current density is uniform and isotropic (constant) within the region $(z' = z - (L_1 + L')\psi,\ \psi)$ for which $P_R \neq 0$ and $P_C \neq 0$,

$$I = \phi_s \int_{\text{all } z,\psi} P_R(z,\psi)\ P_C(z,\psi)\ dzd\psi. \tag{A4}$$

If W_M is the width of the source, we can write

$$\phi_s W_M = i_s, \tag{A5}$$

where i_s is the two dimensional version of the usual three dimensional beam current function. Then

$$I = (i_s/W_M) \int_{\text{all } z,\psi} P_R(z,\psi) P_C(z,\psi) dzd\psi. \tag{A6}$$

There is essentially no approximation so far.

When the collimator slit width $d_C << \text{Min}[W_M, W_R]$ (the usual case), $P_C(z,\psi)$ varies on a small scale with respect to z, in comparison to $P_R(z,\psi)$. We define the collimator slit angular distribution

$$\bar{P}_C(\psi) = \int_{-d_C/2}^{d_C/2} P_C(z,\psi)\ dz/d_C \tag{A7}$$

which is the integral for a single slit of width d_C and normalized so that $\bar{P}_C(\psi = 0) = 1$. Provided that the collimator exit is wider than the penumbra of the beam formed by the source and the rotor aperture,
$W_R + (W_R + W_M)(L' + L_C/2)/L_1$. Hence we may replace $P_C(z,\psi)$ in (A4) with its average value $f_C\bar{P}_C(\psi)$. Then

$$I = \phi_s f_C \int P_R(z,\psi)\ \bar{P}_C(\psi)\ dzd\psi, \tag{A8}$$

where f_C is the fraction of the area of the collimator which is open,

$$f_C = d_C/(d_C + t_C), \tag{A9}$$

and t_C is the thickness of the collimator slats.

We now introduce the rotor aperture angular distribution

$$\bar{P}_R(\psi) = \int_{\text{all } z} P_R(z,\psi)\ dz/W, \tag{A10}$$

which is normalized to a width W which is yet to be chosen. Then

$$I = \phi_s f_C W \int_{all\ \psi} F_R(\psi)\ F_C(\psi)\ d\psi \tag{A11}$$

so that finally,

$$I = i_s f_C (W/W_M) \int_{all\ \psi} F_R(\psi)\ F_C(\psi)\ d\psi. \tag{A12}$$

We now choose W so that $F_R(\psi)$ has the convenient property

$$F_R(\psi)_{max} = 1. \tag{A13}$$

Two cases can be distinguished, $W_R \leq W_M$ and $W_R \geq W_M$, depending on the relative widths of the rotor aperture and the moderator. With reference to Figure A3, we note that the maximum occurs for $\psi = 0$. Then when $W_R \leq W_M$

$$F_R(\psi = 0) = \int P_R(z, \psi = 0)dz/W = W_R/W, \tag{A14}$$

and when $W_R \geq W_M$

$$F_R(\psi = 0) = \int P_R(z, \psi = 0)dz/W = W_M/W. \tag{A15}$$

Therefore to provide in $F_R(\psi)$ the property (A12),

$$W = \begin{cases} W_R \text{ if } W_R \leq W_M \\ W_M \text{ if } W_R \geq W_M. \end{cases} \tag{A16}$$

Hence, from equation (A12), the viewing factor C in equation (1) of the text is

$$C = \begin{cases} W_R/W_M \text{ if } W_R \leq W_M \\ 1 \quad\ \text{if } W_R \geq W_M. \end{cases} \tag{A17}$$

The distinction between the two cases corresponds to whether or not the taking of the absolute value in (18) of the text represents a change in sign of $W_M - W_R$. Otherwise stated, the distinction corresponds to whether a point at the center of the beam lies in the penumbra of the beam (the source is partially obscured by the rotor aperture), or whether the center is in the true umbra of the beam (the source is fully observable through the rotor aperture).

IX. REFERENCES

1. D. L. Price, J. M. Carpenter, C. A. Pelizzari, S. K. Sinha, I. H. Bresof, G. E. Ostrowski, "The IPNS Chopper Spectrometers", Proc. 6th Int. Coll. Advanced Neutron Sources, Argonne, 1982, ICANS-VI, ANL-82-20, 207-214.

2. G. H. Lander and D. L. Price, "Neutron Scattering with Spallation Sources", Physics Today 38 (1985) 38-45.

3. A. D. Taylor, B. C. Boland and Z. A. Bowden, "HET: The High Energy Inelastic Spectrometer at ISIS", Proc. ICANS-IX (Villigen, Switzerland, 1986), SIN report, 349-364 (1987).

4. C.-K. Loong, S. Ikeda and J. M. Carpenter, "The Resolution Function of a Pulsed-Source Neutron Chopper Spectrometer", Nucl. Instr. and Meth. A260 (1987) 381-402.

5. J. M. Carpenter, R. K. Crawford, R. Kleb, C.-K. Loong, G. E. Ostrowski, D. L. Price, M. Nutter, R. Pynn, R. A. Robinson, S. K. Sinha, J. M. Rowe, P. Sokol and A. D. Taylor, LAUR 87-2582 (1987).

6. A. E. Knox, J. M. Carpenter, J. L. Bailey, R. J. Armani, R. N. Blomquist, B. S. Brown, D. R. Henley, A. G. Hins, B. A. Loomis, A. W. Schulke and H. R. Thresh, "Progress on the IPNS Enriched Uranium Booster Target", Proc. ICANS-IX (Villigen, Switzerland, 1986) SIN report, 557-589 (1987).

This work was performed under the auspices of the U.S. Department of Energy, Division of Materials Sciences, Office of Basic Energy Sciences, under Contract W-31-109-ENG-38.